Observability of satellite launcher navigation with INS, GPS, attitude sensors and reference trajectory

Yanick Beaudoin
André Desbiens
Université Laval

Eric Gagnon
DRDC – Valcartier Research Centre

René Landry Jr.
Ecole de Technologie Supérieure

Defence Research and Development Canada

Observability of satellite launcher navigation with INS, GPS, attitude sensors and reference trajectory

Yanick Beaudoin [a,*], André Desbiens [a], Eric Gagnon [b], René Landry Jr. [c]

[a] Département de Génie électrique et de génie Informatique, Université Laval, 1065 Avenue de La Médecine, Québec City, Québec, Canada
[b] Defence Research and Development Canada, 2459 Route de La Bravoure, Québec City, Québec, Canada
[c] Département de génie électrique, École de Technologie Supérieure, 1100 Rue Notre-Dame Ouest, Montréal, Québec, Canada

A B S T R A C T

The navigation system of a satellite launcher is of paramount importance. In order to correct the trajectory of the launcher, the position, velocity and attitude must be known with the best possible precision. In this paper, the observability of four navigation solutions is investigated. The first one is the INS/GPS couple. Then, attitude reference sensors, such as magnetometers, are added to the INS/GPS solution. The authors have already demonstrated that the reference trajectory could be used to improve the navigation performance. This approach is added to the two previously mentioned navigation systems. For each navigation solution, the observability is analyzed with different sensor error models. First, sensor biases are neglected. Then, sensor biases are modelled as random walks and as first order Markov processes.

The observability is tested with the rank and condition number of the observability matrix, the time evolution of the covariance matrix and sensitivity to measurement outlier tests. The covariance matrix is exploited to evaluate the correlation between states in order to detect structural unobservability problems. Finally, when an unobservable subspace is detected, the result is verified with theoretical analysis of the navigation equations.

The results show that evaluating only the observability of a model does not guarantee the ability of the aiding sensors to correct the INS estimates within the mission time. The analysis of the covariance matrix time evolution could be a powerful tool to detect this situation, however in some cases, the problem is only revealed with a sensitivity to measurement outlier test. None of the tested solutions provide GPS position bias observability. For the considered mission, the modelling of the sensor biases as random walks or Markov processes gives equivalent results. Relying on the reference trajectory can improve the precision of the roll estimates. But, in the context of a satellite launcher, the roll estimation error and gyroscope bias are only observable if attitude reference sensors are present.

1. Introduction

The navigation is a critical element of a satellite launcher. Attitude, velocity and position must be known with the best possible precision in order to correct the launcher trajectory. For decades, purely inertial means of navigation were exploited with success [1]. However, inertial navigation estimates are prone to drift. Therefore, high quality units are needed to provide the required precision. Since those units are expensive, aiding sensors are used to reduce the cost and improve precision [1–3]. To ensure that the INS error is reduced by the aiding sensors, the observability of the navigation model must be verified.

For space vehicles, several navigation systems are proposed. Among others, the solution of an INS combined with a GPS receiver is often put forward [4,5] and is considered as usable [1,2,6]. Some tests were also performed on the Space Shuttle and have demonstrated the viability of this solution [7]. However, it is already known that this solution may suffer from observability problems [8–10]. The observability of this approach involves some maneuvers [11–15]. For example, on a system with a low-grade INS and a single-antenna GPS, the gyroscope bias in the direction of the specific force is unobservable if the vehicle moves with constant attitude and acceleration [12]. Another example is the yaw, which is non-observable, during the hovering of a helicopter [16]. In the context of a satellite launcher, the trajectory is optimized to minimize the fuel consumption. That implies that the trajectory is mostly aimed in one direction. Consequently, there is no flexibility to perform the needed maneuvers. Even though the GPS integration type can improve precision

* Corresponding author.
  E-mail address: yanick.beaudoin.1@ulaval.ca (Y. Beaudoin).

Notation

Latines letters

0_i	$i \times i$ zero matrix
$0_{i \times j}$	$i \times j$ zero matrix
A	state matrix
$A1$	propagation of the loosely coupled attitude estimation error into the augmented model
$A2$	closed loop angular dynamics of the launcher
A_{lc}	loosely coupled navigation state matrix
a_m^B	measured acceleration
a_x^B	x-axis component of the body frame acceleration
a_y^B	y-axis component of the body frame acceleration
a_z^B	z-axis component of the body frame acceleration
B	input matrix
$B1$	wind effect input matrix
b_a^B	accelerometer bias
b_g^B	gyroscope bias
B_{lc}	loosely coupled navigation input matrix
b_p^E	GPS position bias
C	output matrix
$C1$ and $C2$	output matrices to compute the difference between the navigation and reference attitudes
c_a	accelerometer bias Markov process time constant
c_g	gyroscope bias Markov process time constant
C_{lc}	loosely coupled navigation output matrix (GPS only)
C_{lc2}	loosely coupled navigation output matrix (GPS and attitude reference sensors)
c_p	GPS position bias Markov process time constant
I_i	$i \times i$ identity matrix
k	time step
n	length of the state vector
s_t	sampling time
T_B^E	rotation matrix from the body frame to the Earth frame
T_E^B	rotation matrix from the Earth frame to the body frame
u	input vector
v_{lc}	loosely coupled navigation output noise vector (GPS only)
v_{lc2}	loosely coupled navigation output noise vector (GPS and attitude reference sensors)
w_{lc}	loosely coupled navigation input vector
x	state vector
$x_i : i \in 1, \cdots, n$	individual component of the state vector
x_a	augmented state vector to compute the difference between the launcher and reference attitudes
x_{lc}	loosely coupled navigation error state vector
y	output vector
y_{lc}	loosely coupled navigation output vector (GPS only)
y_{lc2}	loosely coupled navigation output vector (GPS and attitude reference sensors)

Greek letters

Δa_m^B	accelerometer noise (random walk)
Δb_a^B	accelerometer bias driving noise
Δb_g^B	gyroscope bias driving noise
Δb_p^E	GPS position bias driving noise
$[\Delta \omega_m]_{IB}^B$	rate gyroscope noise (random walk)
$\delta \Psi_e^E$	attitude estimation error
$\Delta \Psi_m^E$	attitude estimation error measurement noise
$\delta \Psi_m^E$	attitude estimation error measurement
$\Delta \Psi_{ref}^B$	difference between the navigation and reference attitudes
$\delta \Psi_{ref}^B$	difference between the launcher and reference attitudes
δr_e^E	position estimation error
Δr_m^E	position estimation error measurement noise
δr_m^E	position estimation error measurement
δv_e^E	velocity estimation error
Δv_m^E	velocity estimation error measurement noise
δv_m^E	velocity estimation error measurement
ω_{IE}^E	angular speed of the Earth rotation
$[\omega_w]_{IB}^B$	angular velocity created by the wind

Subscripts and superscripts

$\{\cdot\}^B$	variable represented in the body frame
$\{\cdot\}^E$	variable represented in the Earth frame

and prevents jamming, it has no influence on the observability [14,17]. Therefore, to simplify the analysis, only the loosely coupled integration is studied. A long lever arm between the INS and the GPS antenna may increase the observability problem [12]. Considering that this aspect has already been evaluated, it will not be treated here and the INS and GPS antenna are considered collocated.

To ensure proper attitude estimation, attitude measurements may be needed [18]. For an airplane, the observability of the INS/GPS combination is not guaranteed unless 3 non-aligned GPS antennas with sufficient lever arm are used [19]. On a helicopter, the yaw observability benefits from the addition of a magnetometer [16]. A star tracker can be employed to solve the attitude observability problem on a space vehicle [20]. It was exploited to improve the INS/GPS precision for the SHEFEX-2 mission [21,22].

The reference trajectory data could be used to increase the navigation solution precision and robustness to GPS outages [23]. The underlying idea of this approach is that, on the launch pad, the attitude of the launcher is perfectly known. As the mission progresses, the confidence that the launcher is following the predicted attitude reduces. If this confidence can be quantified, it allows exploiting the reference trajectory attitude data to better estimate the attitude of the launcher. However, the observability of this approach has been evaluated only with the rank of the observability matrix on a INS/GPS navigation system which neglects the sensor biases.

The addition of attitude reference sensors to an INS can improve the precision by reducing the attitude uncertainties. But it does not provide velocity and position observability [20,24,25]. Since this research is seeking for the observability of all states within the navigation model, the solution combining only these two sensor types is rejected.

Different error models could be exploited depending on the sensors used and the possibility of estimating the sensor errors [26]. With low end sensors, the bias could be a significant source of error. The bias drift of an inertial sensor can be modelled as a first order Markov process [16, 27–29]. A time constant of 100 s is often used [30–32]. However, the time constant could be as long as 1 h [2]. In some cases, when the time constant is of the same order of magnitude as the mission time, the bias is simply modelled as a random walk [11–14,33,34]. The effects of the error model on the observability have not been evaluated before and will be explored in this paper.

The observability is often evaluated with the help of the observability matrix rank [11–15,35]. Unfortunately, only considering the rank of this matrix may not be sufficient. Due to the limited digital precision of computers (around 15 digits with double precision in Matlab®), a near singular matrix might not be detected by the rank of the observability matrix. Therefore, the singular-value decomposition or the condition number of the observability matrix provides a better evaluation of the observability [36]. The order of magnitude of the condition number gives an estimate of the digital precision loss. A rough rule of thumb is that an

increase of 10 in the condition number leads to the loss of one significant digit in the estimates [37].

On the other hand, the time evolution of the estimate covariance matrix gives information which can be overlooked by the observability matrix analysis [11,12,35]. The idea is that the variance of an unobservable (or barely observable) state evolves in the same manner either if the Kalman correction is applied or not. This analysis is highly recommended, if not essential, to evaluate the performance of the Kalman filter [38]. But, with higher order systems, this approach can be cumbersome and relations between states may be difficult to analyze [35]. Fortunately, in the studied cases, the state relationships are evident. Thus, there is no need to rely on more complex techniques, such as evaluating the normalized eigenvalues and eigenvectors of the estimate covariance matrix [35]. The covariance matrix may also be exploited to evaluate the correlation between states. A perfect correlation coefficient (negative or positive) can indicate a structural unobservability, and one should be suspicious of a correlation coefficient which exceeds 0.9 in absolute value [36].

Evaluating the observability of a non-linear system may be complicated. However, the model can be approximated by a piecewise constant model and the observability be evaluated locally for each constant segment

rank and the condition number of the observability matrix. Then, the time evolution of the covariance matrix is exploited to evaluate the observability quality and the ability of the aiding sensors to correct the INS estimates within the mission time. Afterward, the correlation between the states is analyzed to detect structural unobservability. Next, sensitivity to measurement outlier tests are performed to confirm the results obtained from the previous approaches. Finally, unobservable subspaces are investigated with theoretical analysis of the navigation equations.

The paper is structured as follows: section 2 introduces the navigation solutions. Then, the methodology and the observability evaluation technique are presented in section 3. Section 4 shows the observability results obtained with the studied navigation solutions.

2. Navigation solutions

2.1. INS/GPS navigation model

The first navigation solution is an INS aided by a single antenna GPS receiver. The navigation model is the following:

$$
\begin{bmatrix}
\delta\boldsymbol{\Psi}^E_{e\,(k+1)} \\
\delta\boldsymbol{v}^E_{e\,(k+1)} \\
\delta\boldsymbol{r}^E_{e\,(k+1)} \\
\boldsymbol{b}^B_{g\,(k+1)} \\
\boldsymbol{b}^B_{a\,(k+1)} \\
\boldsymbol{b}^E_{p\,(k+1)}
\end{bmatrix}
=
\left[I_{18} + s_t
\begin{bmatrix}
-\boldsymbol{\omega}^E_{IE}\times & 0_3 & 0_3 & -\mathbf{T}^E_{B\,(k)} & 0_3 & 0_3 \\
\left(\mathbf{T}^E_{B\,(k)}\boldsymbol{a}^B_{m\,(k)}\right)\times & -2\boldsymbol{\omega}^E_{IE}\times & 0_3 & 0_3 & \mathbf{T}^E_{B\,(k)} & 0_3 \\
0_3 & I_3 & 0_3 & 0_3 & 0_3 & 0_3 \\
0_3 & 0_3 & 0_3 & -\frac{1}{c_g}I_3 & 0_3 & 0_3 \\
0_3 & 0_3 & 0_3 & 0_3 & -\frac{1}{c_a}I_3 & 0_3 \\
0_3 & 0_3 & 0_3 & 0_3 & 0_3 & -\frac{1}{c_p}I_3
\end{bmatrix}
\right]
\begin{bmatrix}
\delta\boldsymbol{\Psi}^E_{e\,(k)} \\
\delta\boldsymbol{v}^E_{e\,(k)} \\
\delta\boldsymbol{r}^E_{e\,(k)} \\
\boldsymbol{b}^B_{g\,(k)} \\
\boldsymbol{b}^B_{a\,(k)} \\
\boldsymbol{b}^E_{p\,(k)}
\end{bmatrix}
$$

$$
+ s_t
\begin{bmatrix}
-\mathbf{T}^E_{B\,(k)} & 0_3 & 0_3 & 0_3 & 0_3 \\
0_3 & \mathbf{T}^E_{B\,(k)} & 0_3 & 0_3 & 0_3 \\
0_3 & 0_3 & 0_3 & 0_3 & 0_3 \\
0_3 & 0_3 & \sqrt{\frac{2}{c_g s_t}}I_3 & 0_3 & 0_3 \\
0_3 & 0_3 & 0_3 & \sqrt{\frac{2}{c_a s_t}}I_3 & 0_3 \\
0_3 & 0_3 & 0_3 & 0_3 & \sqrt{\frac{2}{c_p s_t}}I_3
\end{bmatrix}
\begin{bmatrix}
[\Delta\boldsymbol{\omega}_m]^B_{IB\,(k)} \\
\Delta\boldsymbol{a}^B_{m\,(k)} \\
\Delta\boldsymbol{b}^B_{g\,(k)} \\
\Delta\boldsymbol{b}^B_{a\,(k)} \\
\Delta\boldsymbol{b}^E_{p\,(k)}
\end{bmatrix}
\tag{1}
$$

[12,14,39–41]. The observability can also be assessed with theoretical analyses of the navigation equation and observability matrix [11–14,39,42].

The first contribution of this work is the observability analysis of four navigation solutions in the context of a satellite launcher mission. The first solution is an INS combined with a single antenna GPS. The second solution adds attitude reference sensors to the INS/GPS couple. For the third approach, the reference trajectory data is added to the INS/GPS couple as suggested in Ref. [23]. The last solution exploits the GPS, INS, attitude reference sensors and the reference trajectory. The observability of the navigation solution with reference trajectory has only been verified with the rank of the observability matrix on a simplified model which includes only the GPS and INS as sensors. In this paper, a more complete evaluation is done using many observability analysis tools and different sensor models.

The second contribution is the evaluation of the effects on the observability of the sensor error equations in the navigation model. Each navigation system is tested with two different sets of inertial sensors. Relatively good sensors are first employed. For these sensors, the bias is considered low enough to be neglected in the navigation model. Then, low quality sensors, which require the bias to be estimated, are used. Modelling sensor biases as a random walk and as a first order Markov process is explored.

For the third contribution, the observability analysis is done using the

$$
\begin{bmatrix}
\delta\boldsymbol{v}^E_{m\,(k)} \\
\delta\boldsymbol{r}^E_{m\,(k)}
\end{bmatrix}
=
\begin{bmatrix}
0_3 & I_3 & 0_3 & 0_3 & 0_3 & 0_3 \\
0_3 & 0_3 & I_3 & 0_3 & 0_3 & I_3
\end{bmatrix}
\begin{bmatrix}
\delta\boldsymbol{\Psi}^E_{e(k)} \\
\delta\boldsymbol{v}^E_{e(k)} \\
\delta\boldsymbol{r}^E_{e(k)} \\
\boldsymbol{b}^B_{g(k)} \\
\boldsymbol{b}^B_{a(k)} \\
\boldsymbol{b}^E_{p(k)}
\end{bmatrix}
+
\begin{bmatrix}
\Delta\boldsymbol{v}^E_{m(k)} \\
\Delta\boldsymbol{r}^E_{m(k)}
\end{bmatrix}
\tag{2}
$$

where $\delta\boldsymbol{\Psi}^E_e$ is the attitude error (rotation angle error vector associated with $\mathbf{T}^E_B$, when considering the body frame perfectly known and the error on the estimated Earth frame, as projected on the real Earth frame [10]), $\delta\boldsymbol{v}^E_e$ is the velocity error and $\delta\boldsymbol{r}^E_e$ is the position error. The vectors $[\Delta\boldsymbol{\omega}_m]^B_{IB}$ and $\Delta\boldsymbol{a}^B_m$ are the rate gyroscope and accelerometer noise vectors and $\mathbf{T}^E_B$ is the attitude rotation matrix from the body frame to the Earth frame, $\boldsymbol{\omega}^E_{IE}$ is the angular speed of the Earth rotation and $\boldsymbol{a}^B_m$ the measured acceleration. The vectors $\boldsymbol{b}^B_g$, $\boldsymbol{b}^B_a$ and $\boldsymbol{b}^E_p$ are the gyroscope, accelerometer and GPS position biases, c_g, c_a and c_p are the corresponding Markov process time constants and $\Delta\boldsymbol{b}^B_g$, $\Delta\boldsymbol{b}^B_a$ and $\Delta\boldsymbol{b}^E_p$ are the corresponding noises. The velocity error $\delta\boldsymbol{v}^E_m$ and position error $\delta\boldsymbol{r}^E_m$ measurements are respectively

affected by the noises $\Delta\boldsymbol{v}_m^E$ and $\Delta\boldsymbol{r}_m^E$. The superscript $\{\cdot\}^E$ and $\{\cdot\}^B$ respectively means that the variable is represented in the Earth frame and the body frame. The sampling time s_t is 0.005 s, k is the time step, 0_i is a $i \times i$ zero matrix and I_i is a $i \times i$ identity matrix.

Different equations can be used to model sensor biases and two of them are tested in this paper. First, biases are modelled by 100 s time constant Markov process, then they are modelled by random walks. To evaluate the effect of modelling the biases as random walks, the shaded terms in equation (1) are set to 0. Then, to remove the different biases, corresponding lines and columns are eliminated. The INS/GPS model is the baseline for all the following models. Therefore, the tests are performed using the same modifications in the upcoming navigation solutions.

2.2. INS/GPS with attitude reference sensor navigation model

Reference attitude sensors add valuable information about the angular motion of the vehicle. Many types of sensors can fulfill the needs of attitude measurement, each with different attributes and weaknesses. Reference attitude sensors might be magnetometers, star trackers, a multi-antenna GPS receiver, etc. Also, combinations of those sensors can be exploited. For the sake of generalization, generic attitude sensors are used in this research. They provide measurements only affected by white noises. To implement these sensors, the only modification needed to the INS/GPS navigation model is the addition of the attitude error measurement $\delta\boldsymbol{\Psi}_m^E$ to equation (2):

$$
\begin{bmatrix} \delta\boldsymbol{\Psi}_{m(k)}^E \\ \delta\boldsymbol{v}_{m(k)}^E \\ \delta\boldsymbol{r}_{m(k)}^E \end{bmatrix} = \begin{bmatrix} I_3 & 0_3 & 0_3 & 0_3 & 0_3 & 0_3 \\ 0_3 & I_3 & 0_3 & 0_3 & 0_3 & 0_3 \\ 0_3 & 0_3 & I_3 & 0_3 & 0_3 & I_3 \end{bmatrix} \begin{bmatrix} \delta\boldsymbol{\Psi}_{e(k)}^E \\ \delta\boldsymbol{v}_{e(k)}^E \\ \delta\boldsymbol{r}_{e(k)}^E \\ \boldsymbol{b}_{g(k)}^B \\ \boldsymbol{b}_{a(k)}^B \\ \boldsymbol{b}_{p(k)}^E \end{bmatrix} + \begin{bmatrix} \Delta\boldsymbol{\Psi}_{m(k)}^E \\ \Delta\boldsymbol{v}_{m(k)}^E \\ \Delta\boldsymbol{r}_{m(k)}^E \end{bmatrix}
$$

(3)

where $\Delta\boldsymbol{\Psi}_m^E$ is the attitude error measurement noise.

2.3. INS/GPS with reference trajectory navigation model

The third navigation solution tested is the INS/GPS with reference

navigation estimates, in which case, the divergence is caused by wrong data being sent to the control. The evolution of the launcher attitude depends on its angular dynamics. Fortunately, the gains scheduling performed in the control to take into account the evolution of the launcher dynamics tends to make the overall control and launcher dynamics constant. Therefore, the closed loop angular dynamics of the launcher can be approximated by a simple linear model. The navigation model is:

$$
\begin{bmatrix} \boldsymbol{x}_{lc(k+1)} \\ \boldsymbol{x}_{a(k+1)} \end{bmatrix} = \begin{bmatrix} A_{lc(k)} & 0_{18\times10} \\ A1_{(k)} & A2_{(k)} \end{bmatrix} \begin{bmatrix} \boldsymbol{x}_{lc(k)} \\ \boldsymbol{x}_{a(k)} \end{bmatrix} + \begin{bmatrix} B_{lc(k)} & 0_{18\times3} \\ 0_{10\times15} & B1_{(k)} \end{bmatrix} \begin{bmatrix} \boldsymbol{w}_{lc(k)} \\ [\boldsymbol{\omega}_w]_{IB(k)}^B \end{bmatrix}
$$

(4)

$$
\begin{bmatrix} \boldsymbol{y}_{lc(k)} \\ \Delta\boldsymbol{\Psi}_{ref(k)}^B \end{bmatrix} = \begin{bmatrix} C_{lc(k)} & 0_{6\times10} \\ C1_{(k)} & C2_{(k)} \end{bmatrix} \begin{bmatrix} \boldsymbol{x}_{lc(k)} \\ \boldsymbol{x}_{a(k)} \end{bmatrix} + \begin{bmatrix} \boldsymbol{v}_{lc(k)} \\ 0_{3\times1} \end{bmatrix}
$$

(5)

where $0_{i\times j}$ is a $i \times j$ zero matrix and:

$$
\boldsymbol{x}_{lc(k+1)} = A_{lc(k)}\boldsymbol{x}_{lc(k)} + B_{lc(k)}\boldsymbol{w}_{lc(k)}
$$

is the compact version of equation (1) of the loosely coupled INS/GPS navigation model and:

$$
\boldsymbol{y}_{lc(k)} = C_{lc(k)}\boldsymbol{x}_{lc(k)} + \boldsymbol{v}_{lc(k)}
$$

the corresponding model output compact version of equation (2). The vector:

$$
\boldsymbol{x}_{a(k)} = \begin{bmatrix} x_{19(k)} \\ x_{20(k)} \\ x_{21(k)} \\ x_{22(k)} \\ x_{23(k)} \\ x_{24(k)} \\ x_{25(k)} \\ \delta\boldsymbol{\Psi}_{ref(k)}^B \end{bmatrix}
$$

represents the difference between the launcher and reference attitudes $\delta\boldsymbol{\Psi}_{ref}^B$ and intermediate states $x_{19}, x_{20}, x_{21}, x_{22}, x_{23}, x_{24}$ and x_{25} needed to compute it. The matrix:

$$
A2_{(k)} = \left[I_{10} + s_t \begin{bmatrix} \begin{bmatrix} -0.5 & 0 & 0 \\ 0 & -6.1248 & 0 \\ 0 & 0 & -6.1248 \end{bmatrix} & \begin{bmatrix} 0 & 0 \\ 5.6922 & 0 \\ 0 & 5.6922 \end{bmatrix} & 0_{3\times2} & -I_3 \\ \begin{bmatrix} 0 & 1 & 0 \\ 0 & 0 & 1 \end{bmatrix} & 0_{2\times2} & 0_{2\times2} & 0_{2\times3} \\ 0_{2\times3} & I_2 & 0_{2\times2} & 0_{2\times3} \\ \begin{bmatrix} 0.6 & 0 & 0 \\ 0 & 30.012 & 0 \\ 0 & 0 & 30.012 \end{bmatrix} & \begin{bmatrix} 0 & 0 \\ 10.7475 & 0 \\ 0 & 10.7475 \end{bmatrix} & \begin{bmatrix} 0 & 0 \\ 0.8111 & 0 \\ 0 & 0.8111 \end{bmatrix} & 0_{3\times3} \end{bmatrix} \right]
$$

trajectory [23]. To perform this, the INS/GPS model, presented in section 2.1, is augmented to estimate the difference between the launcher and reference attitudes. The launcher may diverge from its reference attitude due to unpredictable forces. Wind gusts being the dominant one, it will be the only unpredictable force considered here. However, the model can be easily modified to include other forces. The wind is directly impacting the launcher attitude, but its effect is compensated by the launcher control. The launcher trajectory can also be affected by errors within the

represents the closed loop angular dynamics of the launcher ([23]). The propagation of the loosely coupled attitude estimation error into the augmented model (i.e. how the attitude estimation error affects the launcher angular dynamics) is:

$$
A1_{(k)} = s_t \begin{bmatrix} \boldsymbol{T}_{E(k)}^B & 0_{3\times15} \\ 0_{7\times3} & 0_{7\times15} \end{bmatrix}
$$

where $\mathbf{T_E^B}$ is the attitude rotation matrix from the Earth frame to the body frame. The matrix

$$B1_{(k)} = s_t \begin{bmatrix} 0_{7\times3} \\ I_3 \end{bmatrix}$$

is the wind effect input matrix and $[\boldsymbol{\omega_w}]_{IB}^B$ is the angular velocity created by the wind. The matrix:

$$\begin{bmatrix} C1_{(k)} & C2_{(k)} \end{bmatrix} = \begin{bmatrix} \mathbf{T_{E(k)}^B} & 0_{3\times15} & 0_{3\times7} & I_3 \end{bmatrix}$$

combines the loosely coupled attitude error $\delta\boldsymbol{\Psi}_e^E$ and the difference between the launcher and reference attitudes $\delta\boldsymbol{\Psi}_{ref}^B$ to compute the difference between the navigation and reference attitudes $\boldsymbol{\Delta\Psi}_{ref}^B$.

2.4. INS/GPS with attitude reference sensors and reference trajectory navigation model

The last solution uses the GPS, INS, attitude reference sensors and reference trajectory. As for the solution presented in section 2.2, the only modification needed is integrating the attitude error measurement in the loosely coupled navigation output:

$$\begin{bmatrix} \boldsymbol{y}_{lc2(k)} \\ \boldsymbol{\Delta\Psi}_{ref(k)}^B \end{bmatrix} = \begin{bmatrix} C_{lc2(k)} & 0_{6\times10} \\ C1_{(k)} & C2_{(k)} \end{bmatrix} \begin{bmatrix} \boldsymbol{x}_{lc(k)} \\ \boldsymbol{x}_{a(k)} \end{bmatrix} + \begin{bmatrix} \boldsymbol{v}_{lc2(k)} \\ 0_{3\times1} \end{bmatrix}$$

where:

$$\boldsymbol{y}_{lc2(k)} = C_{lc2(k)}\boldsymbol{x}_{lc(k)} + \boldsymbol{v}_{lc2(k)}$$

is the model output compact version of equation (3).

3. Methodology

The launcher simulator is provided by Defence Research and Development Canada. This non-linear simulator considers, among other things, the launcher flexion, the wind, and the aerodynamic coefficient which varies due to altitude, velocity and aerodynamic angles. The simulated mission is intended to put a satellite on a circular sun-synchronous orbit at an altitude of 500 km. The launch is performed from Churchill, Manitoba in Canada. Only the endoatmospheric phase is evaluated. During this phase, two engines are fired. One during the first 109 s, and the second for the remaining time.

The specifications for the sensors are given in Table 1. The INS specifications are inspired by the IMU-KVH1750 unit from Novatel®. To simulate the higher grade sensors, the biases are simply set to 0. All other parameters are kept identical.

3.1. Observability matrix

Navigation models are varying only due to rotation matrices and acceleration undergone by the launcher. In the context of a satellite launcher, this variation is slow in comparison to the sampling rate, which is 200 Hz. The only exception is when a stage is jettisoned, which lasts for very short periods of time. Furthermore, the sampling rate of all sensors is synchronized with the simulation one. Therefore, most of the time, the

Table 1
Sensors specifications.

GPS receiver	C/A code with wide correlator
Gyroscope random walk	$0.72°/h\sqrt{Hz}$
Gyroscope bias stability	$0.05°/h$
Accelerometer random walk	$117\mu g/\sqrt{Hz}$
Accelerometer bias stability	$7500\mu g$
Attitude reference sensor noise stadard deviation	$1°$

model is changing very slightly between time steps. Considering this, testing the observability at each time step with a piecewise constant model is considered sufficient to evaluate the observability of the navigation models.

The observability is often evaluated using the rank of the observability matrix. Based on the following state space model:

$$\boldsymbol{x}_{(k+1)} = A_{(k)}\boldsymbol{x}_{(k)} + B_{(k)}\boldsymbol{u}_{(k)}$$

$$\boldsymbol{y}_{(k)} = C_{(k)}\boldsymbol{x}_{(k)}$$

where $\boldsymbol{x}$ is the state vector, $\boldsymbol{u}$ is the input vector, $\boldsymbol{y}$ is the output vector and A, B and C are respectively the state, input and output matrices, the observability can be determined by the rank of the observability matrix. The model is locally observable, if the following condition is verified [39,43]:

$$\text{rank} \begin{bmatrix} C_{(k)} \\ C_{(k+1)}A_{(k)} \\ C_{(k+2)}A_{(k+1)}A_{(k)} \\ \vdots \\ C_{(k+n-1)}A_{(k+n-2)}\ldots A_{(k)} \end{bmatrix} = n \tag{6}$$

where n is the length of the state vector. Otherwise, if the rank is lower than the size of the state vector, the system is considered as having a non-observable subspace. To be completely observable, the navigation model must be locally observable for each time steps [39,44]. However, it is delicate to conclude on the complete observability based on local observability [41]. But, having states updated with measurements at each time steps can prevent the estimate errors from growing unbounded [15]. Therefore, only the states which are locally observable all through the mission will be considered as observable.

The evaluation of the observability matrix condition number gives a better insight of the observability. It allows detecting a possible near singular observability matrix, which could be considered as full rank otherwise. The condition number gives a rough estimate of the digital precision loss. A condition number over 10^{10} is considered unacceptable when using double precision variables on a personal computer [37]. The condition number evolves within a simulation, therefore only the maximum value is used. This represents the situation where the navigation is most likely to have an observability weakness.

All navigation solutions are tested with sensor biases represented as Markov processes and random walks. Since Markov process time constants are of the same order of magnitude as the mission time, ignoring them can have a limited impact on estimated standard deviations. For each navigation solution, different combinations of biases are tested to allow detecting which ones are observable. The number of unobservable states detected by the rank of the observability matrix and the condition numbers of the observability matrix are given for each configuration.

3.2. Covariance time evolution analysis

The evolution of the Kalman filter covariance matrix gives information on how estimate uncertainties evolve. Comparing the results obtained with different navigation solutions allows determining the effects of navigation models and aiding sensors. The standard deviation of an estimate that similarly evolves with different models indicates that the corresponding parameters can be omitted (i.e. modelling sensor biases as random walks instead of Markov processes). However, as it will be shown in section 4.1, neglecting terms may affect the rank of the observability matrix.

The observability analysis is defined as determining whether the state vector can be inferred from measurements [15]. Comparing the navigation solutions with different aiding sensors indicates the amount of information provided by the corresponding sensors. Navigation with only an INS is used as a baseline to assess the information provided by aiding

sensors. Its standard deviations are obtained by propagating the covariance matrix based on equation (1). Then, combination of sensors are compared to determine the relative effect of each aiding sensor. In these cases, the standard deviations are extracted from the navigation Kalman filter covariance matrix.

The covariance matrix can be exploited to evaluate the correlation between states. A high correlation coefficient does not automatically indicate a problem. However, it may point out a potential observability issue [36]. For example, if two perfectly correlated states ($x_1 = x_2$) are subtracted in the output equation ($y = x_1 - x_2$), it is impossible to determine their values just by looking at the corresponding output ($y = 0 \forall x_1 = x_2$). But, if they are added ($y = x_1 + x_2$), then their values can be calculated ($x_1 = x_2 = y/2$).

The results obtained with the Kalman filter might be validated using Monte-Carlo simulations. But, if these tests are done without taking into account faulty sensors, the variances obtained with Monte-Carlo simulations can match the theoretical values of the Kalman filter, and that, even if the navigation model has observability weaknesses. Therefore, sensitivity tests are performed by verifying the ability of navigation solutions to correct errors caused by measurement outliers. For example, testing the ability of the navigation filter to correct the effect of a GPS velocity measurement outlier on the GPS position bias estimation (section 4.2.2). In order to compare the behaviour of the navigation filter before and after outliers, these are added at the 50th second of simulation. The choice of the 50th second is also motivated by the fact that it gives enough time for the navigation filter to correct the effect of outliers if the model is observable.

Table 2
Observability vs estimated states. (Shaded values indicate incomplete observability).

	Estimated values				Total number of states	Unobservable states			Condition number		
	Gyroscope biases	Accelerometer biases	GPS position bias	Reference attitude divergence		No bias	Markov process biases	Random walk biases	No bias	Markov process biases [log]	Random walk biases [log]
INS/GPS					9	0			3		
	X						0	0		5	5
		X			12		0	0		5	5
			X				0	3		5	18
	X	X					0	0		5	5
	X		X		15		0	3		5	17
		X	X				0	3		5	17
	X	X	X		18		0	3		5	17
w/ Attitude reference sensors					9	0			0		
	X						0	0		2	2
		X			12		0	0		2	2
			X				0	3		5	18
	X	X					0	0		2	2
	X		X		15		0	3		5	17
		X	X				0	3		5	17
	X	X	X		18		0	3		5	17
INS/GPS/ Reference trajectory				X	19	0			5		
	X			X			0	0		5	5
		X		X	22		0	0		5	5
			X	X			0	3		5	18
	X	X		X			0	0		5	5
	X		X	X	25		0	3		5	18
		X	X	X			0	3		5	18
	X	X	X	X	28		0	3		5	18
w/ Attitude reference sensors				X	19	0			5		
	X			X			0	0		5	5
		X		X	22		0	0		5	5
			X	X			0	3		5	18
	X	X		X			0	0		5	5
	X		X	X	25		0	3		5	18
		X	X	X			0	3		5	18
	X	X	X	X	28		0	3		5	18

4. Result analysis

Navigation models are first evaluated, in section 4.1, using the observability matrix. Section 4.2 verifies the observability with the help of the time evolution of the estimate covariance matrix, the analysis of the correlation between states, and sensitivity to measurement outlier tests.

4.1. Observability using observability matrix

For all configurations, the observability matrix has been evaluated for each time step. Tests showed that the rank of the observability matrix does not change during the mission. The results are summarized in Table 2. Since they are always present, attitude, velocity and position errors are not represented in the table.

When considering the biases as Markov processes, the rank of the observability matrix reveals that all navigation solutions are observable. However, when the sensor biases are modelled as random walks, the estimation of the GPS position bias leads to an unobservable subspace for all navigation solutions. Even if the GPS position bias model has an impact on the rank of the observability matrix, the effect on estimates is negligible (see section 4.2).

The condition number of the observability matrix confirms the results obtained with the rank of the observability matrix. Considering sensor biases as random walks or Markov processes drastically change the order of the condition number when the GPS position bias is estimated (Table 2). In all cases where the rank of the observability matrix reveals an unobservable subspace, the condition number value is at least 10^{17}, otherwise the condition number does not exceed 10^5. As stated in section 3.1, a condition number over 10^{10} is a clear indication of a bad conditioning. Therefore, from the observability matrix rank and condition number standpoint, modelling biases as random walks or Markov processes have an impact on the observability.

On solutions where the reference trajectory is not used and GPS bias is not estimated, the addition of attitude reference sensors reduces the value of the condition number, which can indicate an improved observability. However, on navigation solutions where the reference trajectory is exploited, the addition of attitude reference sensors has no effect on the condition number. However, as it will be shown in sections 4.2.3 and 4.2.4, the attitude reference sensors improve the observability either if the reference trajectory is used or not.

The analysis of equation (2) shows that the position error and the GPS bias are not affecting other states within the state vector. For the solutions where the reference trajectory is used (equation (4)), only the attitude error $\delta\boldsymbol{\Psi}_e^E$ is affecting the vector $\boldsymbol{x}_a$ through the matrix $A1$. Considering that $\delta\boldsymbol{r}_e^E$ and $\boldsymbol{b}_p^E$ are not affecting other states, their

observability can be analyzed with a simplified model.

From equation (1), the propagation of the position error and the GPS position bias is:

$$\begin{bmatrix} \delta\boldsymbol{r}_{e(k+1)}^E \\ \boldsymbol{b}_{p(k+1)}^E \end{bmatrix} = \left[I_6 + s_t \begin{bmatrix} 0_3 & 0_3 \\ 0_3 & -\dfrac{1}{c_p}I_3 \end{bmatrix} \right] \begin{bmatrix} \delta\boldsymbol{r}_{e(k)}^E \\ \boldsymbol{b}_{p(k)}^E \end{bmatrix} + s_t \begin{bmatrix} 0_3 \\ \sqrt{\dfrac{2}{c_p s_t}}I_3 \end{bmatrix} \begin{bmatrix} \Delta\boldsymbol{b}_{p(k)}^E \end{bmatrix}$$

and based on equation (2), the corresponding output equation is:

$$\begin{bmatrix} \delta\boldsymbol{r}_{m(k)}^E \end{bmatrix} = \begin{bmatrix} I_3 & I_3 \end{bmatrix} \begin{bmatrix} \delta\boldsymbol{r}_{e(k)}^E \\ \boldsymbol{b}_{p(k)}^E \end{bmatrix} + \begin{bmatrix} \Delta\boldsymbol{r}_{m(k)}^E \end{bmatrix} \tag{7}$$

which gives the following observability matrix:

$$\begin{bmatrix} I_3 & I_3 \\ I_3 & I_3\left(1 - \dfrac{s_t}{c_p}\right) \\ I_3 & I_3\left(1 - \dfrac{s_t}{c_p}\right)^2 \\ I_3 & I_3\left(1 - \dfrac{s_t}{c_p}\right)^3 \\ I_3 & I_3\left(1 - \dfrac{s_t}{c_p}\right)^4 \\ I_3 & I_3\left(1 - \dfrac{s_t}{c_p}\right)^5 \end{bmatrix}$$

The observability matrix is full rank only if $\frac{s_t}{c_p}\neq 0$, and the condition number of the simplified model observability matrix is proportional to c_p as presented in Fig. 1. The limit case when $c_p\rightarrow\infty$, is equivalent to model the bias as a random walk. Therefore, weak observability problems should be expected as c_p increases. It should be noted that for the studied mission, c_p is within the same range as the mission time. In this case, the Markov process is close to a random walk, which can lead to observability weaknesses.

4.2. Observability using the time evolution of the covariance matrix

4.2.1. Observability analysis using INS/GPS

To begin, the observability of the INS/GPS solution with none of the biases estimated is analyzed. In section 4.1, the rank of the observability matrix indicates that all states are observable and the order of the condition number, which is 3, can be considered small [37]. Therefore, from the observability matrix standpoint, no observability problems should be expected. But, as already mentioned in Ref. [23], it can be seen from Fig. 2 that GPS measurements barely improve the roll error estimate. Even with ideal GPS measurements ($\Delta\boldsymbol{v}_m^E = 0_{3\times 1}$ and $\Delta\boldsymbol{r}_m^E = 0_{3\times 1}$ in equation (2)), the estimated roll error standard deviation is within the same range as when the INS is used alone (Fig. 2). It is demonstrated that the attitude error parallel to the acceleration is unobservable [12,13]. If the launcher is moving in a perfect straight line solely in the forward direction, any rotation about the body frame roll axis leads to the same velocity and position measurements. Therefore, a roll estimation error cannot be detected using the GPS measurement unless the launcher undergoes lateral acceleration. Theoretically, from equation (1) the propagation of the velocity estimation error is:

$$\delta\boldsymbol{v}_{e(k+1)}^E = \delta\boldsymbol{v}_{e(k)}^E + s_t\left(\mathbf{T}_{B(k)}^E\boldsymbol{a}_{m(k)}^B \times \delta\boldsymbol{\Psi}_{e(k)}^E - 2\omega_{IE}^E \times \delta\boldsymbol{v}_{e(k)}^E + \mathbf{T}_{B(k)}^E\boldsymbol{b}_{a(k)}^B \\ + \mathbf{T}_{B(k)}^E\Delta\boldsymbol{a}_{m(k)}^B\right)$$

Only considering the terms related to the propagation of the attitude

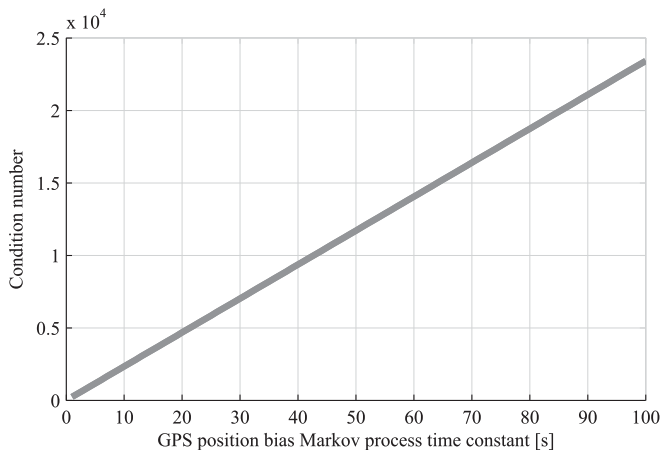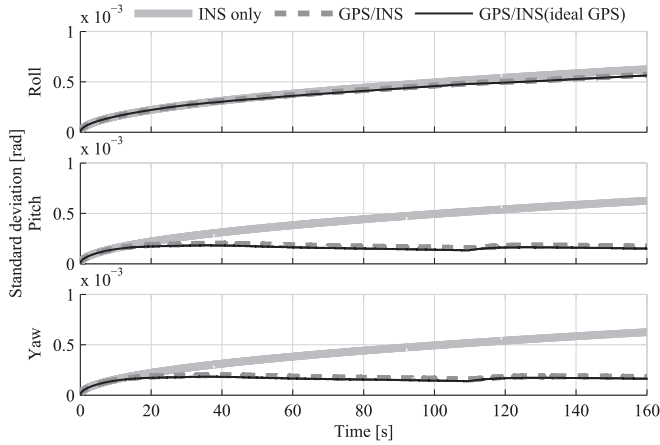**Fig. 1.** Condition number of the simplified model observability matrix vs GPS position bias Markov process time constant.

Fig. 2. Time evolution of estimated attitude error standard deviations.

Fig. 3. Time evolution of estimated GPS position bias standard deviations.

estimation error into the velocity estimation error gives:

$$\delta v^E_{e(k+1)} = \delta v^E_{e(k)} + s_t \mathbf{T}^E_{\mathbf{B}(k)} a^B_{m(k)} \times \delta \Psi^E_{e(k)} + \cdots$$

which represented in the body frame is:

$$\delta v^B_{e(k+1)} = \delta v^B_{e(k)} + s_t a^B_{m(k)} \times \delta \Psi^B_{e(k)} + \cdots$$

with:

$$a^B_{m(k)} \times = \begin{bmatrix} 0 & -a^B_z & a^B_y \\ a^B_z & 0 & -a^B_x \\ -a^B_y & a^B_x & 0 \end{bmatrix}$$

where a^B_x, a^B_y and a^B_z are the individual components of the body frame acceleration vector. If the lateral acceleration is null (i.e. $a^B_y = 0$ and $a^B_z = 0$) the first component of $\delta \Psi^B_{e(k)}$, which is the body frame roll estimation error, is not propagated into the velocity estimation error. Considering that the launcher lateral acceleration is almost null, the roll estimation error has little impact on the velocity estimation error. The position estimation error is also barely affected, since computed from the velocity estimation error. Therefore, the roll estimation error is weakly observable and additional sensors are needed to ensure proper observability of all states.

4.2.2. Observability analysis using INS/GPS with attitude reference sensors

The second approach analyzed is the INS/GPS with attitude reference sensors. The theoretical analysis of the observability matrix in section 4.1 demonstrates that an observability problem occurs when the GPS position bias is modelled as a random walk. However, the evolution of the covariance matrix shows that standard deviations of the GPS position bias are greatly reduced by the use of aiding sensors (Fig. 3). Furthermore, modelling the GPS position bias as a random walk or a Markov process has no effect on standard deviations, which is in contradiction with the observability results obtained with the rank and condition number of the observability matrix in section 4.1. To verify the observability of the GPS position bias, when modelled as a Markov process, an outlier is added to the velocity measurement vector provided by the GPS. A 3 m/s bias outlier is added on the 3 velocity components at the 50th second of the simulation. Although the GPS position bias is well estimated before the occurrence of the outlier, a static error remains afterward (Fig. 4). This confirms that the GPS position bias is weakly observable, even when modelled as a Markov process. But, the GPS position error, including the bias, can be approximated by a white noise [38]. Considering this, the GPS position bias estimation should be removed from the navigation model and the variance of the position
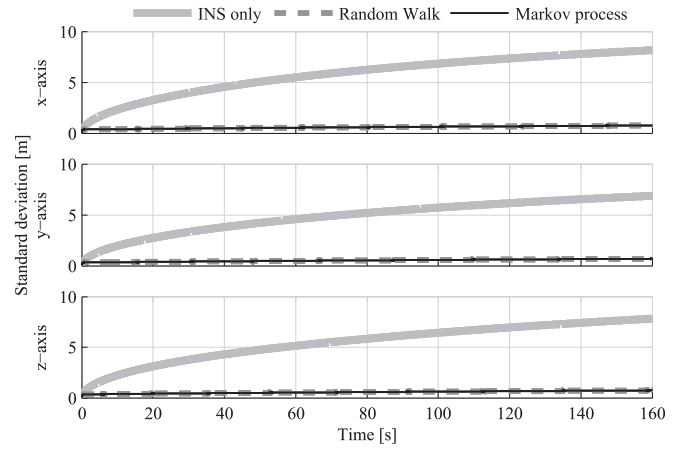
error measurement noise adjusted accordingly.

Considering biases as Markov processes or random walks has a negligible impact on estimated standard deviations of accelerometer and GPS position biases. However, gyroscope bias standard deviations are greatly affected (Fig. 5). It should be noted that sensor biases are modelled by Markov processes for the navigation with only the INS, which explains why it outperforms the INS/GPS solution with biases modelled by random walks.

In view of these results, one might think that gyroscope biases are unobservable. Strictly speaking, this is not an observability problem. However, the effect on the estimates is similar. Even on a fully observable model, the ability of correcting estimates can be affected by sensor noises [40]. In fact, the space mission flight time is short and biases do not grow to the point where their estimation can benefit from attitude reference sensor measurements. But, as the quality of gyroscopes becomes lower, the improvement provided by aiding sensors becomes obvious, as it can be seen in Fig. 6, where the gyroscope bias stability specification is multiplied by 1000. Also, the effect of sensor bias models becomes less evident. This highlights the importance of considering the observability analysis along with the relative precision of sensors.

4.2.3. Observability analysis using INS/GPS with and without reference trajectory

The next test compares the INS/GPS solutions with and without the reference trajectory as additional information. Fig. 7 shows that the standard deviation of the roll estimate error is greatly reduced by the
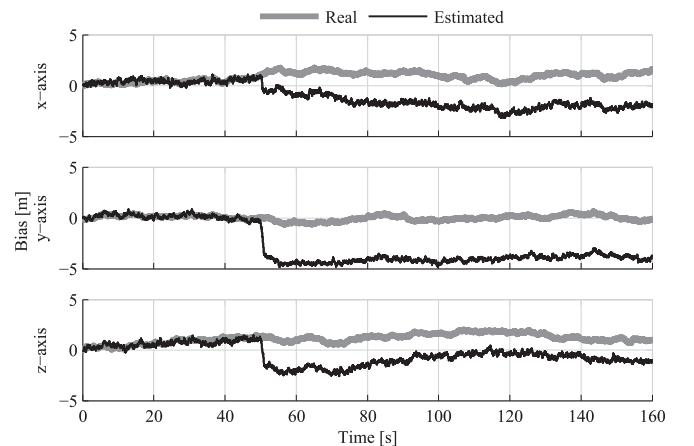

Fig. 4. Time evolution of the GPS position bias when a 3 m/s bias outlier is added on the 3 velocity components at the 50th second of the simulation.
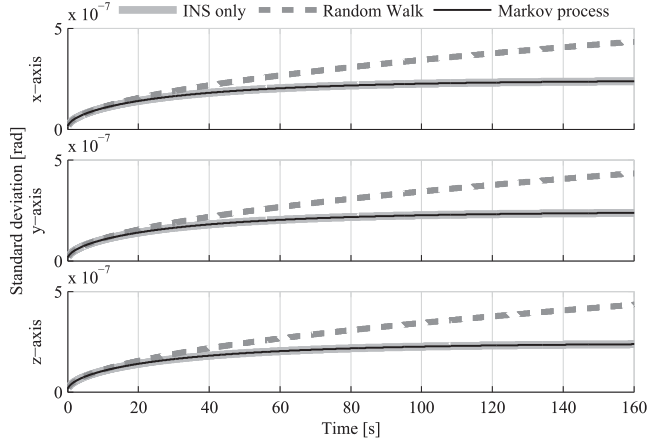
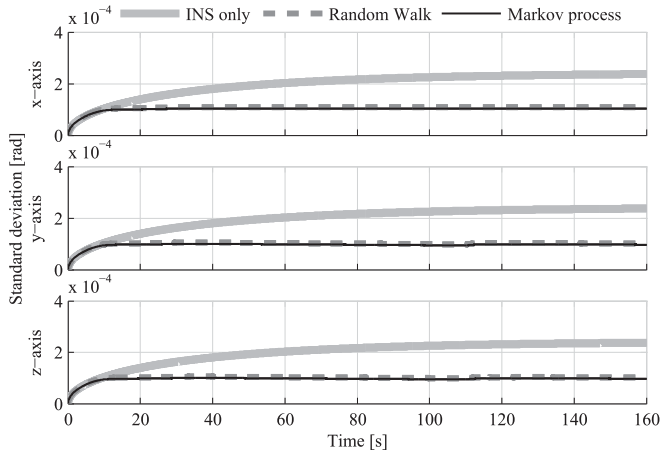Fig. 5. Time evolution of estimated gyroscopes bias standard deviations.

Fig. 6. Time evolution of gyroscope bias standard deviations with bias stability multiplied by 1000.
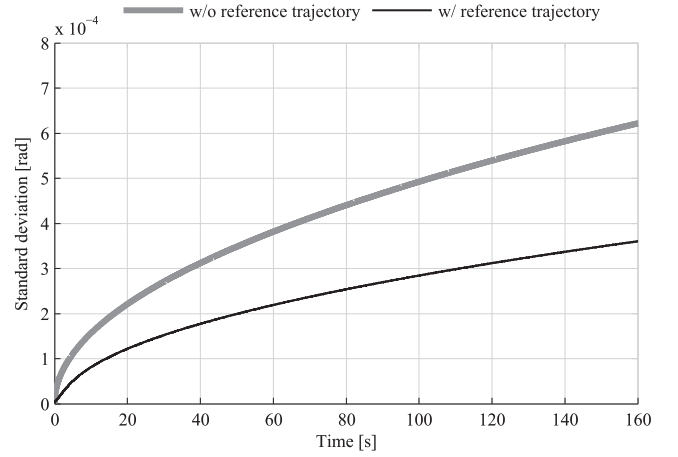

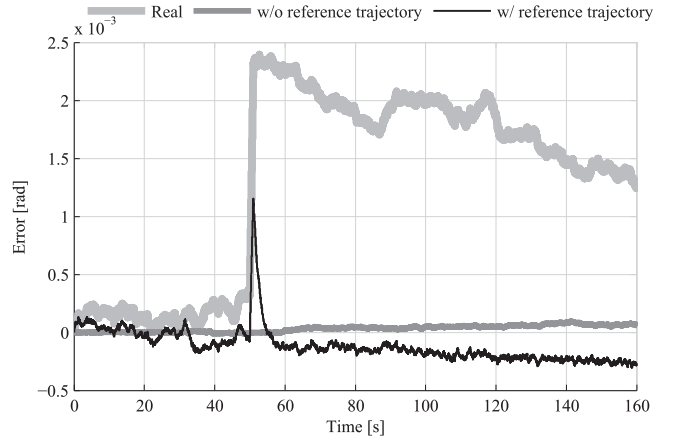Fig. 7. Time evolution of the estimated roll error standard deviation.

Fig. 8. Time evolution of the roll error with a 0.002 rad/s gyroscope measurement outlier on the roll axis at the 50th second of simulation.
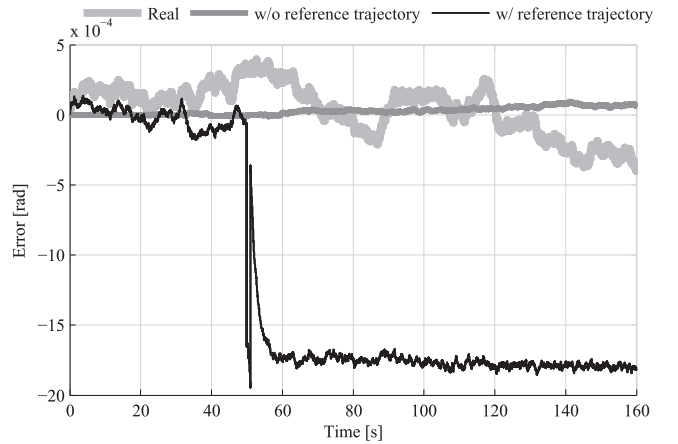

Fig. 9. Time evolution of the roll error with a 0.002 rad/s outlier on the roll component of the reference trajectory at the 50th second of simulation.

addition of the reference trajectory. However, all the other estimations are not improved. Even if the roll estimation is better, the observability problem of the INS/GPS solution is still present when the reference trajectory is used. If an outlier is added to roll rate measurements (0.002 rad/s at the 50th second), both solutions exhibit a static error on the roll error estimate (Fig. 8). The solution which makes use of the reference trajectory could be affected by an outlier on the reference trajectory data too. Fig. 9 presents the effect of a 0.002 rad/s outlier on the reference roll value at the 50th second. Obviously, the solution which does not use the reference trajectory data is unaffected.

An analysis of the correlation between states for the INS/GPS solution with the reference trajectory reveals a near perfect negative correlation between attitude estimation error and launcher divergence from the reference attitude when both are represented in the same reference frame. Fig. 10 shows the time evolution of the correlation coefficients during the first 5 s of the mission. This is due to the fact that the effect of the wind on the rotational motion of the launcher is low. Therefore, the launcher divergence from its reference attitude is mainly caused by the attitude estimation error. Also, the rotational dynamics of the launcher is faster than the evolution of the attitude estimation error, hence during normal operation $\mathbf{T}_{E(k)}^{B}\delta\mathbf{\Psi}_{e(k)}^{E} \approx -\delta\mathbf{\Psi}_{ref(k)}^{B}$. In equation (5), these two values are added:

$$\mathbf{\Delta\Psi}_{ref(k)}^{B} = \mathbf{T}_{E(k)}^{B}\delta\mathbf{\Psi}_{e(k)}^{E} + \delta\mathbf{\Psi}_{ref(k)}^{B} \tag{8}$$

consequently:

$$\mathbf{\Delta\Psi}_{ref(k)}^{B} \approx 0_{3\times1} \quad \forall \quad \mathbf{T}_{E(k)}^{B}\delta\mathbf{\Psi}_{e(k)}^{E} \approx -\delta\mathbf{\Psi}_{ref(k)}^{B}$$

Since $\delta\mathbf{\Psi}_{ref}^{B}$ does not affect other states within the model and is only measured through equation (8), to uniquely determine the value of $\delta\mathbf{\Psi}_{e}^{E}$ and $\delta\mathbf{\Psi}_{ref}^{B}$, $\delta\mathbf{\Psi}_{e}^{E}$ must be observable. Unfortunately, the roll estimation error is weakly observable (section 4.2.1). Consequently, this navigation
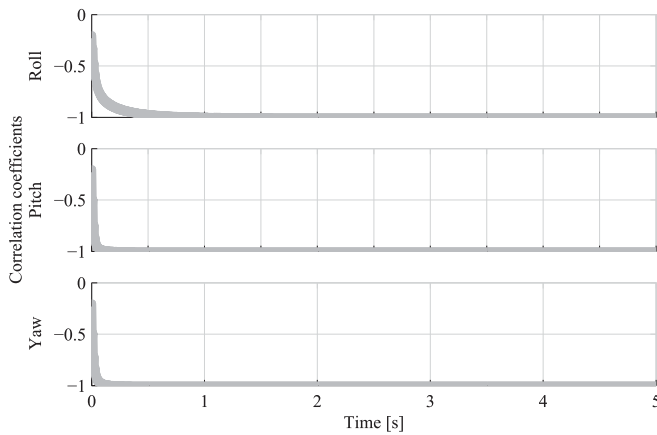
Fig. 10. Time evolution of the correlation coefficients between the attitude error and launcher divergence from its reference trajectory.
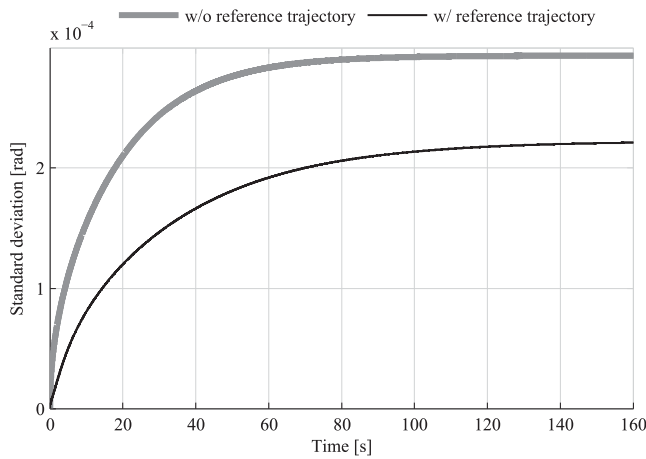

Fig. 11. Time evolution of the estimated roll error standard deviation.

Fig. 12. Time evolution of the roll error with a 0.002 rad/s gyroscope measurement outlier on the roll axis at the 50th second of simulation.

Fig. 13. Time evolution of the launcher divergence from its reference trajectory (roll) with a 0.002 rad/s gyroscope measurement outlier on the roll axis at the 50th second of simulation.

solution suffers from structural unobservability [36].

To explain the fast change of attitude error estimates at the moment of the outlier, it should be noted that the difference between the navigation and the reference attitude is perfectly known. Therefore, the value of $\Delta\Psi_{ref}^B$ change instantaneously due to the outlier. The presence of equation (8) in the Kalman filter measurement of residual makes corrections be applied to $\delta\Psi_e^E$ and $\delta\Psi_{ref}^B$. But, since components in the body roll axis of $\delta\Psi_e^E$ and $\delta\Psi_{ref}^B$ are weakly observable, both values do not necessarily converge to the real values.

The use of the reference trajectory reduces the roll estimation error. However, this approach does not improve the observability and can be sensitive to outliers within the reference trajectory data. Consequently, the uses of the reference trajectory cannot be recommended when exploited with only an INS and a GPS.

4.2.4. Observability analysis using INS/GPS/attitude reference sensors with and without reference trajectory

The last test compares the INS/GPS/attitude reference sensor solutions with and without the reference trajectory. As when no attitude sensors are present (section 4.2.3), only the roll estimation is improved with the help of the reference trajectory as additional information. Fig. 11 shows that the roll estimation with attitude reference sensors can be improved with the help of the reference trajectory. When adding a 0.002 rad/s gyroscope outlier on the roll rate at the 50th second of the simulation, both solutions are able to correct the roll error estimation.

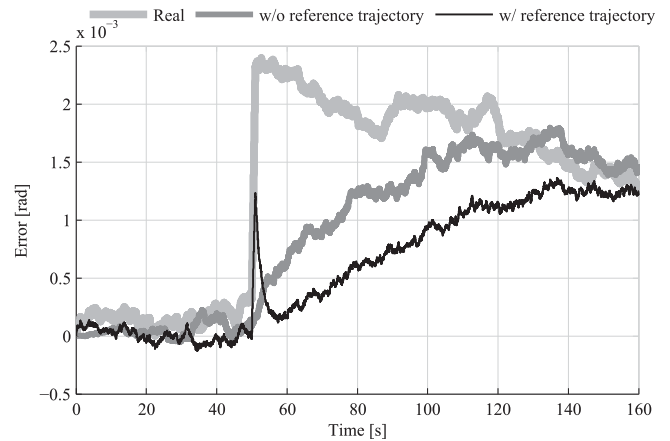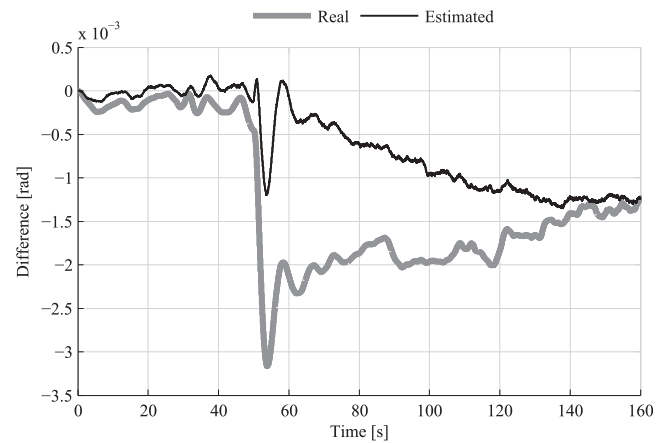Even if both approaches are able to correct the effect of the outlier

within the same time range, the one exploiting the reference trajectory initially captures the effect faster, but is then slower to correct it. Again, this is due to the near perfect negative correlation between the attitude error estimates and the estimation of the gap between launcher and reference attitudes. As shown in section 4.2.3, at the exact moment of the outlier occurrence, the reference trajectory data helps to rectify the attitude estimation. But after that, the negative correlation makes the attitude estimation error (Fig. 12) and difference between launcher and reference attitude (Fig. 13) to be underestimated. However, unlike the previous solution (section 4.2.3), attitude reference sensors provide the needed measurements to overcome the structural unobservability problem. Consequently, the uses of the reference trajectory to reduce the roll estimation error can be recommended when attitude reference sensors are present.

As stated in section 4.1, the improved observability provided by attitude reference sensors to the solution which exploit the reference trajectory is not revealed by the rank and condition number of the observability matrix. This highlights the importance of not relying solely on the observability matrix to assess the observability of a model.

5. Conclusion

In this paper the observability of four navigation solutions for a satellite launcher is evaluated. For each navigation solution, three different sensor error models are tested. First, it is demonstrated that one could not

rely solely on the rank of the observability matrix to assess the observability. The analysis of the condition number of the observability matrix gives a better insight of the observability and helps to detect a near singular observability matrix. The covariance matrix time evolution allows determining the contribution of aiding sensors to reduce INS estimation errors. Therefore, it delivers precious information on possible weak observability. The analysis of the correlation between states may also reveal structural unobservability. However, in some cases, a sensitivity analysis is required to detect observability problems.

In the context of a satellite launcher, the results show that:

- None of the suggested navigation solutions provide GPS position bias observability. Consequently, this bias should be removed from the navigation model and its effect considered within the position error measurement noise.
- Roll estimation error and gyroscope bias are only observable if attitude reference sensors are present. Therefore, the addition of these sensors is recommended.
- Relying on the reference trajectory data into the navigation solution does not improve the observability. However, it allows reducing the standard deviation of the roll estimation, which makes this approach interesting when combined with attitude reference sensors.
- Modelling biases as Markov processes or random walks is barely affecting the navigation performances. Therefore, for the studied cases, both models can be used for the gyroscope and accelerometer biases.
- The observability may be affected by the quality of the sensors through the choice of sensor error models. But the relative precision of sensors should also be taken into account. In fact, if INS aiding sensors do not provide accurate enough measurements, the results attained can be similar to those without aiding sensors. Strictly speaking, the inability of correcting estimates within the mission time is not an unobservability problem, but it creates similar behaviours.

A next step could be to simplify the navigation solution which makes use of the reference trajectory to consider only the divergence of the launcher from its reference trajectory into the body roll axis. This change should not affect the improvement provided by this approach, but it will reduce the amount of data needed and the computational load.

Acknowledgements

References

[1] S. Narmada, P. Delaux, A. Biard, Use of GNSS for next european launcher generation, in: Proceedings of the 6th International ESA Conference on Guidance, Navigation and Control Systems, Noordwijk, Netherlands, 2006, p. 9.

[2] W. Ma, Y. Xu, Y. Bao, B. Yang, Autonomous integrated navigation plan for space transfer vehicle, in: 2nd International Symposium on Systems and Control in Aerospace and Astronautics (ISSCAA), Piscataway, NJ, USA, 2008, pp. 1–6, https://doi.org/10.1109/ISSCAA.2008.4776342.

[3] G.T. Schmidt, INS/GPS Technology Trends, Tech. Rep. RTO-EN-SET-116(2010), North Atlantic Treaty Organization, 2010.

[4] H. Zhang, W. Zheng, G. Tang, Stellar/inertial integrated guidance for responsive launch vehicles, Aerosp. Sci. Technol. 18 (2012) 35–41, https://doi.org/10.1016/j.ast.2011.04.003.

[5] S. Belin, J.F. Averlant, F. Dubuc, S. Villers, A. Reis, Requirements toward GNSS chain for ariane 5 mid-life evolution, in: 2010 5th ESA Workshop on Satellite Navigation Technologies and European Workshop on GNSS Signals and Signal Processing (NAVITEC), 2010, pp. 1–8, https://doi.org/10.1109/NAVITEC.2010.5708078.

[6] L. Wang, P. Ye, C. Zhai, Z. Y, High performance strapdown inertial navigation system algorithms for space flight, in: 2nd International Symposium on Systems and Control in Aerospace and Astronautics (ISSCAA), Piscataway, NJ, USA, 2008, pp. 1–5, https://doi.org/10.1109/ISSCAA.2008.4776315.

[7] B. Willms, Space integrated GPS/INS (SIGI) navigation system for space shuttle, in: Gateway to the New Millennium. 18th Digital Avionics Systems Conference. Proceedings (Cat. No.99CH37033), Vol. 2, Piscataway, NJ, USA, 1999, pp. 7–14, https://doi.org/10.1109/DASC.1999.821988.

[8] J. Waldmann, Feedforward ins aiding: an investigation of maneuvers for in-flight alignment, Controle Autom. 18 (4) (2007) 459–470.

[9] F.A. Faruqi, K.J. Turner, Extended kalman filter synthesis for integrated global positioning/inertial navigation system, Appl. Math. Comput. 115 (2–3) (2000) 213–227, https://doi.org/10.1016/S0096-3003(98)10068-1.

[10] P.G. Savage, Strapdown Analytics, Strapdown Associates, Inc, 2007.

[11] I. Rhee, M.F. Abdel-Hafez, J.L. Speyer, Observability of an integrated GPS/INS during maneuvers, Aerosp. Electron. Syst. IEEE Trans. 40 (2) (2004) 526–535, https://doi.org/10.1109/TAES.2004.1310002.

[12] S. Hong, M.H. Lee, H.H. Chun, S.H. Kwon, J.L. Speyer, Observability of error states in GPS/INS integration, IEEE Trans. Veh. Technol. 54 (2) (2005) 731–742, https://doi.org/10.1109/TVT.2004.841540.

[13] M. Lee, S. Hong, M. Lee, S. Kwon, H.H. Chun, Observability analysis of alignment errors in GPS/INS, J. Mech. Sci. Technol. 19 (6) (2005) 1253–1267, https://doi.org/10.1007/BF02984046.

[14] Y. Tang, Y. Wu, M. Wu, W. Wu, X. Hu, L. Shen, INS/GPS integration: global observability analysis, Veh. Technol. IEEE Trans. 58 (3) (2009) 1129–1142, https://doi.org/10.1109/TVT.2008.926213.

[15] I. Klein, Y. Bar-Shalom, I. Rusnak, Observability analysis for tracking of coordinated turn maneuvers, in: Electrical Electronics Engineers in Israel (IEEEI), 2014 IEEE 28th Convention of, 2014, pp. 1–5, https://doi.org/10.1109/EEEI.2014.7005784.

[16] M. Barczyk, M. Jost, D. Kastelan, A. Lynch, K. Listmann, An experimental validation of magnetometer integration into a GPS-aided helicopter UAV navigation system, in: American Control Conference (ACC), 2010, 2010, pp. 4439–4444, https://doi.org/10.1109/ACC.2010.5530999.

[17] D.H. Hwang, D.W. Lim, S.L. Cho, S.J. Lee, Unified approach to ultra-tightly-coupled GPS/INS integrated navigation system, Aerosp. Electron. Syst. Mag. IEEE 26 (3) (2011) 30–38, https://doi.org/10.1109/MAES.2011.5746183.

[18] M. Samaan, S. Theil, Development of a low cost star tracker for the SHEFEX mission, Aerosp. Sci. Technol. 23 (2012) 469–478, https://doi.org/10.1016/j.ast.2011.09.013. http://www.sciencedirect.com/science/article/pii/S1270963811001684.

[19] J.F. Wagner, G. Kasties, Applying the principle of integrated navigation systems to estimating the motion of large vehicles, Aerosp. Sci. Technol. 8 (2) (2004) 155–166, https://doi.org/10.1016/j.ast.2003.09.006. http://www.sciencedirect.com/science/article/pii/S1270963803000981.

[20] T. Tanabe, M. Harigae, Experimental validation of GPS-INS-STAR hybrid navigation system for space autonomy, Acta Astronaut. 21 (5) (1990) 295–308, https://doi.org/10.1016/0094-5765(90)90090-8.

[21] S. Theil, M. Schlotterer, M. Hallmann, M. Conradt, Hybrid navigation system for the SHEFEX-2 mission, in: Guidance, Navigation and Control Conference and Exhibit, No. AIAA 2008-6991, AIAA, Honolulu, HI, USA, 2008.

[22] S. Theil, S. Steffes, M. Samaan, M. Conradt, M. Markgraf, I. Vanschoenbeek, Hybrid navigation system for spaceplanes, launch and re-entry vehicles, in: 16th International Space Planes and Hypersonic Systems and Technologies Conference, No. AIAA 2009-7381, AIAA/DLR/DGLR, Bremen, Germany, 2009.

[23] Y. Beaudoin, A. Desbiens, E. Gagnon, R. Landry, Improved satellite launcher navigation performance by using the reference trajectory data, in: Proceeding of International Navigation Conference 2015 (INC15), Royal Institute of Navigation, Manchester Conference Center, UK, 2015.

[24] J. Ali, F. Jiancheng, SINS/ANS integration for augmented performance navigation solution using unscented kalman filtering, Aerosp. Sci. Technol. 10 (3) (2006) 233–238, https://doi.org/10.1016/j.ast.2005.11.009.

[25] J. Ali, Z. Changyun, F. Jiancheng, An algorithm for astro-inertial navigation using CCD star sensors, Aerosp. Sci. Technol. 10 (5) (2006) 449–454, https://doi.org/10.1016/j.ast.2006.01.004.

[26] T. Grigorie, I.R. Lungu, M. Edu, R. Obreja, Concepts for error modeling of miniature accelerometers used in inertial navigation systems, in: Annals of the University of Craiova, Electrical Engineering vol. 34, 2010.

[27] W. Flenniken, J. Wall, D. Bevly, Characterization of various IMU error sources and the effect on navigation performance, in: Proceedings of the 18th International Technical Meeting of the Satellite Division of the Institute of Navigation (ION GNSS 2005), ION GNSS, Long Beach, CA, 2005, pp. 967–978.

[28] J.H. Wall, D.M. Bevly, Characterization of inertial sensor measurements for navigation performance analysis, in: Proceedings of the 19th International Technical Meeting of the Satellite Division of the Institute of Navigation (ION GNSS 2006), Fort Worth, TX, USA, 2006, pp. 2678–2685.

[29] A. Noureldin, T.B. Karamat, M.D. Eberts, A. El-Shafie, Performance enhancement of MEMS-based INS/GPS integration for low-cost navigation applications, IEEE Trans. Veh. Technol. 58 (3) (2009) 1077–1096, https://doi.org/10.1109/TVT.2008.926076.

[30] N. El-Sheimy, Emerging MEMS IMU and its impact on mapping applications, in: D. Fritsch (Ed.), Photogrammetric Week, Stuttgart, Germany, 2009.

[31] O.J. Woodman, An Introduction to Inertial Navigation, Tech. Rep. UCAM-CL-TR-696, University of Cambridge, Computer Laboratory, 2007.

[32] W.S. Flenniken, Modeling Inertial Measurement Units and Analyzing the Effect of Their Errors in Navigation Applications, Auburn University, 2005. Ph.D. thesis.

[33] L. Shuang, P. Yuming, Radio beacons/IMU integrated navigation for mars entry, Adv. Space Res. 47 (7) (2011) 1265–1279, https://doi.org/10.1016/j.asr.2011.01.001. http://www.sciencedirect.com/science/article/pii/S0273117711000251.

[34] H. Chang, L. Xue, W. Qin, G. Yuan, W. Yuan, An integrated MEMS gyroscope array with higher accuracy output, Sensors 8 (4) (2008) 2886–2899, https://doi.org/10.3390/s8042886. http://www.mdpi.com/1424-8220/8/4/2886.

[35] F.M. Ham, R.G. Brown, Observability, eigenvalues, and kalman filtering, aerospace and electronic systems, IEEE Trans. AES 19 (2) (1983) 269–273, https://doi.org/10.1109/TAES.1983.309446.

[36] M.S. Grewal, A.P. Andrews, Kalman Filtering Theory and Practice Using MATLAB, second ed., Electronic and electrical engineering, Wiley, New York, 2001. http://www3.interscience.wiley.com/cgi-bin/booktoc/94515619.

[37] K.L. Judd, Numerical Methods in Economics, MIT Press, 1998.

[38] M.S. Grewal, L.R. Weill, A.P. Andrews, Global Positioning Systems, Inertial Navigation, John Wiley, New York, 2001 integration, http://www3.interscience.wiley.com/cgi-bin/booktoc/89012356Ω, http://ariane.ulaval.ca/cgi-bin/recherche.cgi?qu=a1447204.

[39] Z. Chen, Local observability and its application to multiple measurement estimation, IEEE Trans. Ind. Electron. 38 (6) (1991) 491–496, https://doi.org/10.1109/41.107106.

[40] D. Goshen-Meskin, I.Y. Bar-Itzhack, Observability analysis of piece-wise constant systems. part 1: Theory, IEEE Trans. Aerosp. Electron. Syst. 28 (4) (1992) 1056–1067, https://doi.org/10.1109/7.165367.

[41] H.J. Marquez, Nonlinear Control Systems, John Wileyiley & sons, 2003.

[42] J. Farrell, Aided Navigation : GPS with High Rate Sensors, McGraw-Hill, 2008.

[43] K. Shen, A.V. Proletarsky, K.A. Neusypin, Quantitative analysis of observability in linear time-varying systems, in: 2016 35th Chinese Control Conference (CCC), 2016, pp. 44–49, https://doi.org/10.1109/ChiCC.2016.7553058.

[44] A.P. Sage, Optimum Systems Control, Prentice Hall, 1968.

Eric Gagnon received B.E. and Ph.D. degrees in electrical engineering from Université Laval, Quebec City (Canada), in 1991 and 1999, respectively. He worked for three years as an electrical engineer in the R&D industry, seven years as a research professional in academia and fifteen years as a defense scientist at Defence Research and Development Canada. He is specialized in guidance, navigation and control of weapons.
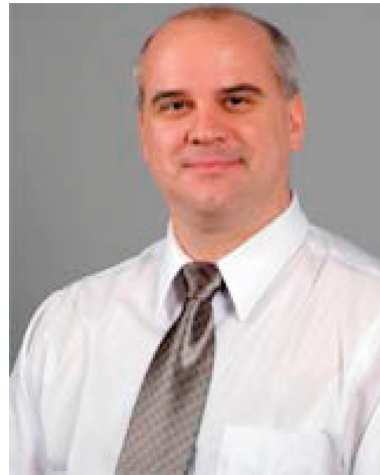
René Jr Landry received an electrical engineering degree at École Polytechnique of Montreal in 1992, a Master of Science in Satellite Communication engineering in 1993, a DEA in microwave in 1994 and a Ph.D. in GNSS anti-jamming at SupAero in 1998. Since 1999, he is professor at the department of electrical engineering at École de Technologie Supérieure (ÉTS), and the director of LASSENA laboratory. His expertise in embedded systems, navigation and avionic is applied notably in the field of transport, aeronautic, and space technologies.

Yanick Beaudoin is a Ph.D. student at Université Laval, Québec City, Canada. He completed his Bachelor in 2009 and his Master in 2012, both in electrical engineering at Université Laval. His research interest is the navigation of satellite launchers.

André Desbiens is a Professor at the Department of Electrical and Computer Engineering at Université Laval, Québec City, Canada. He has been a faculty member since 1995. He completed his Ph.D. (Electrical Engineering) in 1995 and his undergraduate studies (Engineering Physics) in 1988, both at Université Laval. His research interests lie in the area of guidance, navigation and control and also in industrial process control and real-time optimization.

DOCUMENT CONTROL DATA

(Security markings for the title, abstract and indexing annotation must be entered when the document is Classified or Designated)

1. ORIGINATOR (The name and address of the organization preparing the document. Organizations for whom the document was prepared, e.g., Centre sponsoring a contractor's report, or tasking agency, are entered in Section 8.) DRDC – Valcartier Research Centre Defence Research and Development Canada 2459 route de la Bravoure Quebec (Quebec) G3J 1X5 Canada	2a. SECURITY MARKING (Overall security marking of the document including special supplemental markings if applicable.) CAN UNCLASSIFIED 2b. CONTROLLED GOODS NON-CONTROLLED GOODS DMC A

3. TITLE (The complete document title as indicated on the title page. Its classification should be indicated by the appropriate abbreviation (S, C or U) in parentheses after the title.)

Observability of satellite launcher navigation with INS, GPS, attitude sensors and reference trajectory

4. AUTHORS (last name, followed by initials – ranks, titles, etc., not to be used)

Beaudoin, Yanick; Desbiens, André; Gagnon, Eric; Landry, René Jr.

5. DATE OF PUBLICATION (Month and year of publication of document.) November 2017	6a. NO. OF PAGES (Total containing information, including Annexes, Appendices, etc.) 12	6b. NO. OF REFS (Total cited in document.) 44

7. DESCRIPTIVE NOTES (The category of the document, e.g., technical report, technical note or memorandum. If appropriate, enter the type of report, e.g., interim, progress, summary, annual or final. Give the inclusive dates when a specific reporting period is covered.)

External Literature (P)

8. SPONSORING ACTIVITY (The name of the department project office or laboratory sponsoring the research and development – include address.)

DRDC – Valcartier Research Centre
Defence Research and Development Canada
2459 route de la Bravoure
Quebec (Quebec) G3J 1X5
Canada

9a. PROJECT OR GRANT NO. (If appropriate, the applicable research and development project or grant number under which the document was written. Please specify whether project or grant.)	9b. CONTRACT NO. (If appropriate, the applicable number under which the document was written.)
10a. ORIGINATOR'S DOCUMENT NUMBER (The official document number by which the document is identified by the originating activity. This number must be unique to this document.) DRDC-RDDC-2017-P110	10b. OTHER DOCUMENT NO(s). (Any other numbers which may be assigned this document either by the originator or by the sponsor.) Acta Astronautica 142 (2018) 277–288

11a. FUTURE DISTRIBUTION (Any limitations on further dissemination of the document, other than those imposed by security classification.)

Public release

11b. FUTURE DISTRIBUTION OUTSIDE CANADA (Any limitations on further dissemination of the document, other than those imposed by security classification.)

12. ABSTRACT (A brief and factual summary of the document. It may also appear elsewhere in the body of the document itself. It is highly desirable that the abstract of classified documents be unclassified. Each paragraph of the abstract shall begin with an indication of the security classification of the information in the paragraph (unless the document itself is unclassified) represented as (S), (C), (R), or (U). It is not necessary to include here abstracts in both official languages unless the text is bilingual.)

The navigation system of a satellite launcher is of paramount importance. In order to correct the trajectory of the launcher, the position, velocity and attitude must be known with the best possible precision. In this paper, the observability of four navigation solutions is investigated. The first one is the INS/GPS couple. Then, attitude reference sensors, such as magnetometers, are added to the INS/GPS solution. The authors have already demonstrated that the reference trajectory could be used to improve the navigation performance. This approach is added to the two previously mentioned navigation systems. For each navigation solution, the observability is analyzed with different sensor error models. First, sensor biases are neglected. Then, sensor biases are modelled as random walks and as first order Markov processes.

The observability is tested with the rank and condition number of the observability matrix, the time evolution of the covariance matrix and sensitivity to measurement outlier tests. The covariance matrix is exploited to evaluate the correlation between states in order to detect structural unobservability problems. Finally, when an unobservable subspace is detected, the result is verified with theoretical analysis of the navigation equations.

The results show that evaluating only the observability of a model does not guarantee the ability of the aiding sensors to correct the INS estimates within the mission time. The analysis of the covariance matrix time evolution could be a powerful tool to detect this situation, however in some cases, the problem is only revealed with a sensitivity to measurement outlier test. None of the tested solutions provide GPS position bias observability. For the considered mission, the modelling of the sensor biases as random walks or Markov processes gives equivalent results. Relying on the reference trajectory can improve the precision of the roll estimates. But, in the context of a satellite launcher, the roll estimation error and gyroscope bias are only observable if attitude reference sensors are present.

_____

13. KEYWORDS, DESCRIPTORS or IDENTIFIERS (Technically meaningful terms or short phrases that characterize a document and could be helpful in cataloguing the document. They should be selected so that no security classification is required. Identifiers, such as equipment model designation, trade name, military project code name, geographic location may also be included. If possible keywords should be selected from a published thesaurus, e.g., Thesaurus of Engineering and Scientific Terms (TEST) and that thesaurus identified. If it is not possible to select indexing terms which are Unclassified, the classification of each should be indicated as with the title.)

Observability, INS, GPS, reference trajectory